# Design of L2<sub>1</sub>-type antiferromagnetic semiconducting full-Heusler compounds: A first principles DFT + GW study

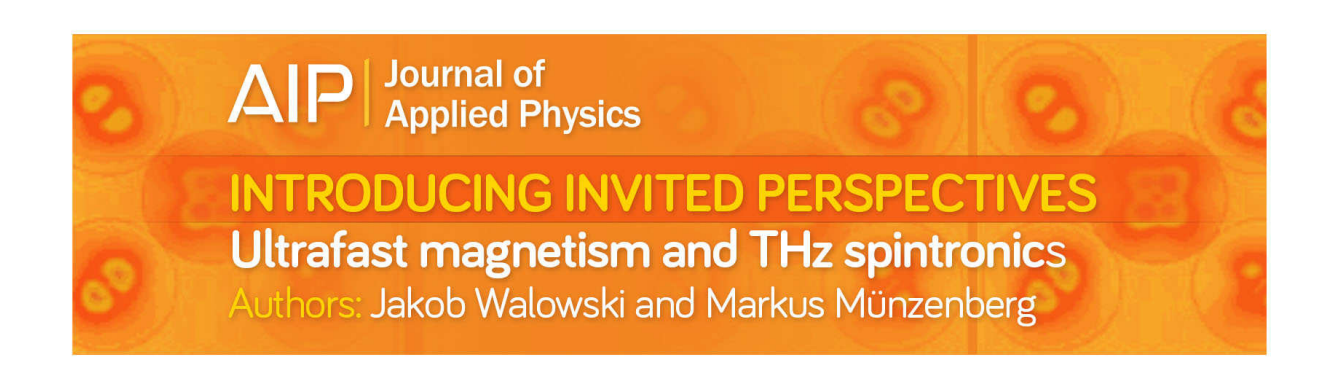
M. Tas, E. Şaşıoğlu, C. Friedrich, S. Blügel, and I. Galanakis

Citation: J. Appl. Phys. 121, 053903 (2017); doi: 10.1063/1.4975351

View online: http://dx.doi.org/10.1063/1.4975351

View Table of Contents: http://aip.scitation.org/toc/jap/121/5

Published by the American Institute of Physics







# Design of $L2_1$ -type antiferromagnetic semiconducting full-Heusler compounds: A first principles DFT + GW study

M. Tas, <sup>1,a)</sup> E. Şaşıoğlu, <sup>2,b)</sup> C. Friedrich, <sup>2</sup> S. Blügel, <sup>2</sup> and I. Galanakis <sup>1,c)</sup>
<sup>1</sup>Department of Materials Science, School of Natural Sciences, University of Patras, GR-26504 Patra, Greece
<sup>2</sup>Peter Grünberg Institut and Institute for Advanced Simulation, Forschungszentrum Jülich and JARA, 52425 Jülich, Germany

(Received 22 December 2016; accepted 20 January 2017; published online 6 February 2017)

Antiferromagnetic spintronics is an on-going growing field of research. Employing both standard density functional theory and the *GW* approximation within the framework of the full-potential linearized augmented-plane-wave method, we study the electronic and magnetic properties of seven potential antiferromagnetic semiconducting Heusler compounds with 18 (or 28 when Zn is present) valence electrons per unit cell. We show that in these compounds G-type antiferromagnetism is the ground state and that they are all either semiconductors (Cr<sub>2</sub>ScP, Cr<sub>2</sub>TiZn, V<sub>2</sub>ScP, V<sub>2</sub>TiSi, and V<sub>3</sub>Al) or semimetals (Mn<sub>2</sub>MgZn and Mn<sub>2</sub>NaAl). The many-body corrections have a minimal effect on the electronic band structure with respect to the standard electronic structure calculations. *Published by AIP Publishing*. [http://dx.doi.org/10.1063/1.4975351]

# I. INTRODUCTION

Among the subfields of spintronics, the so-called "antiferromagnetic spintronics" is constantly growing during recent years. 1,2 This new research field deals with the implementation of antiferromagnetic semiconductors in conventional spintronic devices either as a substitute to the ferromagnetic materials or in heterostructures with the latter, e.g., in spin torque-transfer (STT) magnetic memories.<sup>2</sup> Antiferromagnetic semiconductors have also been proposed in order to control the properties of magnetic topological insulators unveiling new avenues towards dissipationless topological antiferromagnetic spintronics. Antiferromagnets, contrary to ferromagnets, create vanishing stray fields leading to minimal energy losses. On the other hand, the current-control of the magnetic information stored in antiferromagnetic materials still needs to be studied in depth.<sup>1,2</sup> Main challenges in the antiferromagnetic spintronics involve their coherent growth on top of ferromagnets, like in the STT memories, and the discovery of antiferromagnets with high Néel temperature (T<sub>N</sub>) is requested for realistic devices since most have  $T_N$  far below the room temperature.<sup>2</sup>

Heusler compounds are playing a central role in the development of spintronics and magnetoelectronics. A,5 These ternary and quaternary intermetallic compounds present a large variety of magnetic behaviors and their magnetic properties are implicitly connected to their electronic properties. Although several studies have been devoted to Heusler compounds (for a review see Refs. 10 and 11), the ongoing research reveals new properties with potential interest for applications. Among them, there are *ab-initio* studies which have identified few Heusler compounds exhibiting zero net magnetization. The latter are made of magnetic constituents and are usually defined as half-metallic fully compensated ferrimagnets (also known as half-metallic antiferromagnets), 12,13

The large number of possible combinations of chemical elements in Heusler compounds leads unavoidably to the conclusion that it could be feasible to identify also antiferromagnetic semiconductors among them. Such materials would combine the large critical temperature usually exhibited by Heusler compounds to the coherent growth on top of other ferromagnetic Heusler compounds since most of them crystallize in the same cubic structure. Motivated by the experimental detection of the antiferromagnetic semiconducting behavior in V<sub>3</sub>Al, a Heusler compound with 18 valence electrons crystallizing in the  $D0_3$  lattice structure, we search for other potential antiferromagnetic semiconducting Heusler compounds with 18 valence electrons per unit cell. We identified six candidates Cr<sub>2</sub>ScAl, Cr<sub>2</sub>TiZn, Mn<sub>2</sub>NaAl, Mn<sub>2</sub>MgZn, V<sub>2</sub>ScP, and V<sub>2</sub>TiSi. Cr<sub>2</sub>TiZn and Mn<sub>2</sub>MgZn have actually 28 valence electrons due to the presence of the Zn atom. But Zn's 3d orbitals are completely occupied creating isolated bands low in energy and, thus, can be considered semicore states not affecting the studied properties. Therefore, we will refer to them as 18valence electron compounds as well. We should note finally that, as it is well-known for half-metallic or magnetic semiconducting Heusler compounds, the substitution of an element by an isovalent one (i.e., same number of valence electrons) does not alter the electronic and the magnetic properties of the compounds, since the latter depend on the total number of valence electrons in the unit cell. <sup>7-9</sup> Thus, e.g., Mn<sub>2</sub>LiAl and Mn<sub>2</sub>KAl show similar properties as Mn<sub>2</sub>NaAl.

# **II. COMPUTATIONAL METHOD**

We have performed simulations of the electronic and magnetic properties of the six compounds and  $V_3Al$  using

c)Electronic mail: galanakis@upatras.gr



and Cr<sub>2</sub>CoGa, which belongs to this class of materials, has been successfully grown. However, these materials are metals, and at finite temperature, the atomic spin magnetic moments are not compensated anymore leading to usual ferrimagnetic behavior. Thus, such materials do not fulfil the requirements for antiferromagnetic spintronics.

a)Electronic mail: tasm236@gmail.com

b)Present address: Institut für Physik, Martin-Luther-Universität Halle-Wittenberg, D-06099 Halle (Saale), Germany.

the density-functional theory (DFT) based on the fullpotential linearized augmented-plane-wave (FLAPW) method as implemented in the FLEUR code<sup>17</sup> within the generalized gradient approximation (GGA) of the exchange-correlation potential as parameterized by Perdew, Burke, and Ernzerhof (PBE). 18 Since such calculations are restricted to the groundstate properties and often fail in describing the band gap of semiconductors, we have also employed the GW approximation using the PBE results as input to perform one-shot GW calculations using the Spex code. <sup>19</sup> Details of the calculations are identical to the ones in Ref. 20, where non-magnetic semiconducting Heusler compounds were studied. Also, since our calculations refer to the zero-temperature ground-state, the description of the magnetic properties at finite temperatures could be more complicated; e.g., for V<sub>3</sub>Al, the longitudinal spin-fluctuations play a decisive role in the formation of the vanadium magnetic moments.<sup>21</sup>

Prior to presenting our results in Sec. III, we should also discuss the possibility of growing experimentally the compounds under study. V<sub>3</sub>Al is the only one that has been grown experimentally in the cubic Heusler structure as a film<sup>22</sup> confirming the predictions of Skaftouros et al. in Ref. 23; note that the stable lattice structure of V<sub>3</sub>Al is the A15, and V<sub>3</sub>Al in this structure is a well-known superconductor.<sup>24</sup> Searching the Open Quantum Materials Database we found that all other compounds under study, with the exception of V<sub>2</sub>ScP, can exist experimentally although the cubic  $L2_1$  lattice structure is not the most stable phase; in the case of the V-Sc-P phase diagram, no ternary compound was suggested to exist. 25,26 Thus, we expect that modern growth instruments and techniques would allow the successful growth of the compounds under study in the present article as was recently the case of the quaternary antiferromagnetic semiconducting Heusler (CrV)TiAl. For the latter, its existence was suggested using ab-initio calculations in Ref. 27, and recently Stephen and collaborators have grown it in the form a film confirming also its theoretically predicted antiferromagnetic semiconducting character.28

### **III. RESULTS AND DISCUSSION**

We begin our discussion by presenting the ground state properties as obtained by the PBE calculations. The compounds under study have the formula  $X_2YZ$  and crystallize

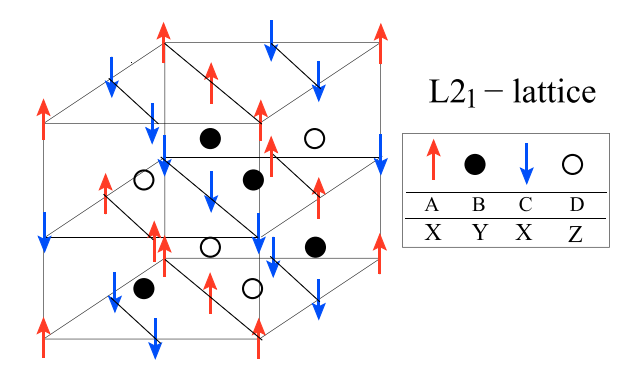


FIG. 1. Schematic representation of the  $L2_1$  lattice structure. For the two inequivalent X atoms, we also demonstrate the direction of the spin magnetic moments in the antiferromagnetic configuration.

in the  $L2_1$  cubic lattice structure, which is presented in Fig. 1. It is actually an fcc lattice with four atoms as basis along the diagonal: X atoms at the A and C sites at (0 0 0) and  $(\frac{1}{2}, \frac{1}{2}, \frac{1}{2})$ , Y atoms at the B site at  $(\frac{1}{4}, \frac{1}{4}, \frac{1}{4})$ , and Z atoms at the D  $(\frac{3}{4}, \frac{3}{4}, \frac{3}{4})$  site. The exchange constants of the 3d-transition metals obey the semi-phenomenological Slater-Bethe-Néel curve, which predicts antiferromagnetism for the early transition metals with less than half-filled shells, like V, Cr, and Mn, for small interatomic distances. <sup>29,30</sup> In the compounds under study the X atoms at the A and C sites are second neighbors and their distance is exactly half the lattice constant as can be seen in Fig. 1. This value is for all compounds under study slightly larger than 3 Å, as we can deduce from the lattice constants presented in Table I, and is not far away from the 2.52 Å which is the distance between the Cr atoms in the antiferromagnetic bcc Cr. Thus, we expect for the compounds under study that the X atoms at the A and C sites show an antiferromagnetic coupling of their spin magnetic moments. Assuming that the ground state is the G-type antiferromagnetic state shown in Fig. 1,16 we first determined the equilibrium lattice constants using total energy calculations. The obtained results are presented in the first column of Table I. Lattice constants in all cases exceed 6 A, nearly reaching 6.5 Å for Mn<sub>2</sub>MgZn. We then established the stability of the antiferromagnetic state by performing calculations where we imposed our systems to be either non-magnetic or ferromagnetic. We note that we could not get ferromagnetic ground-states for V<sub>2</sub>TiSi and V<sub>3</sub>Al.

TABLE I. PBE calculated lattice constants,  $a_{eq}$  in Å (we published the value for  $V_3Al$  in Ref. 16), and difference of the total energies (in eV) between the antiferromagnetic (AFM) and non-magnetic (NM) states,  $\Delta E^{AFM-NM}$ , as well as the difference between the AFM and ferromagnetic (FM) configurations,  $\Delta E^{AFM-FM}$ . The AFM state is the ground state in all cases. The other columns present the PBE calculated spin magnetic moments in  $\mu_B$  for the Heusler compounds under study in the AFM case. We also present in parenthesis the results for the FM coupling of the spin magnetic moments. We use the symbols A and C to denote the two transition metal atoms sitting at different sites. For  $V_2$ TiSi and  $V_3$ Al, we could not get a FM solution irrespective of the starting distribution of the atomic spin magnetic moments. Note that both the energy differences and the total spin magnetic moments are given per formula unit.

$X_2YZ$	$a_{\rm eq}({ m \AA})$	$\Delta E^{AFM\text{-}NM}$	$\Delta E^{AFM\text{-}FM}$	$m^{X(A)}$	$m^{X(C)}$	$m^{ m Y}$	$m^{\mathbb{Z}}$	$m^{ ext{total}}$
Cr <sub>2</sub> ScAl	6.39	-1.946	-0.756	3.306 (2.677)	-3.306 (2.677)	0 (0.255)	0 (-0.086)	0 (5.522)
Cr <sub>2</sub> TiZn	6.14	-1.162	-0.829	2.918 (2.380)	-2.918(2.380)	0(-0.018)	0 (0.019)	0 (4.761)
Mn <sub>2</sub> NaAl	6.45	-2.831	-0.162	3.867 (3.671)	-3.867(3.671)	0(-0.006)	0(-0.217)	0 (7.119)
$Mn_2MgZn$	6.23	-2.310	-0.130	3.582 (3.296)	-3.582(3.296)	0(-0.061)	0(-0.115)	0 (6.415)
V <sub>2</sub> ScP	6.17	-0.692	-0.552	2.155 (1.405)	-2.155(1.405)	0 (0.488)	0(-0.026)	0 (3.272)
V <sub>2</sub> TiSi	6.10	-0.379		1.776	-1.776	0	0	0
V <sub>3</sub> Al	6.09	-0.131	•••	1.384	-1.384	0	0	0



In the second column of Table I, we present the difference in total energy between the antiferromagnetic and the non-magnetic states. The minus sign implies that the antiferromagnetic state is more favorable. V<sub>3</sub>Al shows the smallest energy difference of 0.131 eV. For the Cr- and Mn-based compounds, the energy difference is one order of magnitude larger, so the magnetic state is considerably more stable. In the third column, we present the difference in total energy between the antiferromagnetic and the ferromagnetic configurations calculated at the equilibrium lattice constant. For the Cr-based compounds, the energy difference shows a pretty large value of about  $-0.8 \,\mathrm{eV}$  in favor of the antiferromagnetic configuration, while in the Mn-based compounds, it is much smaller -0.13 and  $-0.16\,\mathrm{eV}$ . The value of  $-0.13 \,\mathrm{eV}$  is almost identical to that of  $V_3 Al$  for which the Néel temperature  $(T_{\rm N})$  has been calculated to be 988 K, <sup>16</sup> and thus for the rest of the compounds we expect significantly larger T<sub>N</sub> values making the antiferromagnetism a very robust property of the compounds under study even at elevated temperatures.

In Table I, we present the atomic spin magnetic moments in  $\mu_{\rm B}$  for both the antiferromagnetic and the ferromagnetic configurations; the latter in parenthesis. In the G-type antiferromagnetism case presented in Fig. 1, consecutive (111) planes of X atoms have antiparallel moments, and the Y and Z atoms exhibit a zero spin magnetic moment due to symmetry reasons, i.e., they are surrounded by four X atoms sitting at A sites with positive and four X atoms at C sites with negative spin magnetic moments. The absolute values of the atomic spin magnetic moments of the X atoms are pretty high exceeding even 3.5  $\mu_B$  in the case of the Mn atoms. These values are significantly larger than the corresponding spin magnetic moments in the ferromagnetic case. The total spin magnetic moment for all antiferromagnetic compounds is exactly zero. This is compatible with the appearance of semiconducting behavior, although it does not guarantee it, as we will discuss later on.

We briefly discuss the atom-resolved electronic properties. In Fig. 2, we present the density of states (DOS) for all studied compounds. In the case of the V- and Cr-based compounds, the orbitals of the Y atoms have a significant weight in the same region as the d-orbitals of the X atoms (V or Cr), and thus hybridization is pretty strong. On the contrary, in the case of the two Mn-based compounds, the situation is clearly different. Occupied Mn d-orbitals are almost of a unique spin character due to the larger exchange splitting, and thus they are located much lower in energy, leading to a localization of the spin magnetic moment similar to other

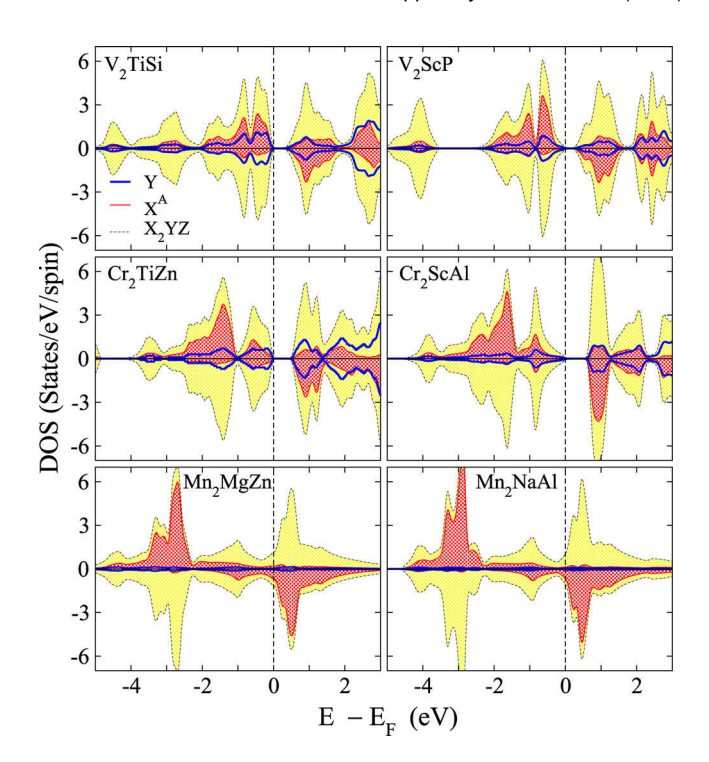


FIG. 2. Atom-resolved and total DOS for the  $X_2YZ$  compounds under study. The zero energy value corresponds to the Fermi level. Positive (negative) DOS values correspond to the spin-up (spin-down) electrons.

Mn-based Heusler compounds.<sup>31</sup> Simultaneously, the Y atoms (Mg or Na) have vanishing weight in the energy region of the Mn d orbitals. Thus, hybridization is very weak in the Mn<sub>2</sub>MgZn and Mn<sub>2</sub>NaAl compounds.

Next, we focus on the calculation of the electronic band structure of the compounds under study as well as the determination of the energy band gaps and of the transition energies. For the GW calculations, we have used an  $8\times8\times8$  grid to carry out the calculations, which is dense enough to accurately reproduce the band structure as shown also in Ref. 20. We present all obtained energy values within both the PBE and the GW approximations in Table II. Moreover, in Fig. 3 we present, as an example, the band structure for  $V_2TiSi$  along the high symmetry lines in the Brillouin zone using both PBE and GW. The band structures of the other compounds look similar.

Prior to the discussion of the results, we note that all compounds studied have 18 valence electrons, 9 per spin direction; thus the hybridization scheme is similar to that of  $V_3A$  in Ref. 16. In the case of semiconducting behavior, the gap is created between the occupied triple-degenerate  $t_{2g}$  orbitals obeying both the octahedral and tetrahedral symmetry

TABLE II. Calculated PBE (in parenthesis) and GW energy band gaps and transition energies (all in eV) between certain high-symmetry points for the antiferromagnetic semiconducting Cr- and V-based studied materials.

Compound	$\mathrm{E}_\mathrm{g}^{GW}~(\mathrm{E}_\mathrm{g}^\mathrm{PBE})$	$\Gamma  ightarrow \Gamma$	$X \rightarrow X$	$\Gamma \to X$	$X \to \Gamma$
Cr <sub>2</sub> ScAl	0.893 (0.674)	1.242 (1.143)	2.212 (1.676)	1.032 (0.882)	2.422 (1.938)
Cr <sub>2</sub> TiZn	0.800 (0.586)	1.782 (1.681)	1.417 (1.028)	1.062 (1.079)	2.137 (1.630)
$V_2ScP$	0.034 (0.123)	0.034 (0.123)	1.995 (2.124)	1.383 (1.350)	0.646 (0.897)
V <sub>2</sub> TiSi	0.427 (0.383)	1.935 (1.984)	1.736 (1.871)	1.344 (1.350)	2.328 (2.506)
$V_3Al$	0.065 (0.081)	2.159 (2.320)	1.575 (1.185)	1.171 (1.079)	2.563 (2.426)



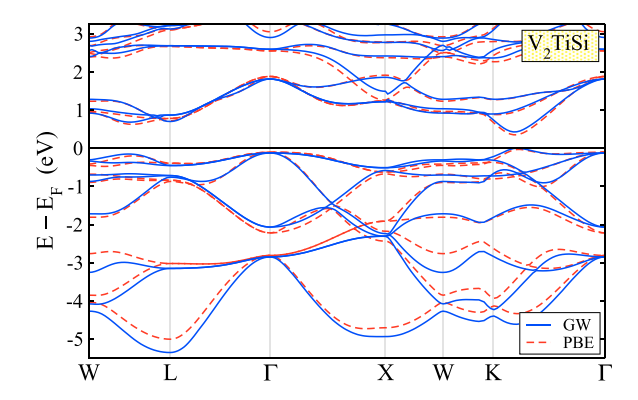


FIG. 3. Calculated electronic band structure of  $V_2$ TiSi along the high-symmetry directions in the first Brillouin zone using either the PBE (red dashed line) or the GW (blue solid line) approximations. The zero energy value denotes the Fermi level.

groups and being extended over all X and Y sites, and the triple-degenerate  $t_{1u}$  orbitals obeying exclusively the octahedral symmetry and thus being located only at the X atoms.

We start our presentation of the electronic properties with the three V based compounds. All three compounds are G-type antiferromagnetic semiconductors as can be deduced from their total DOS shown in Fig. 2. The band structure of V<sub>2</sub>TiSi is presented in Fig. 3 where we observe that overall PBE and GW present a qualitatively similar band structure picture especially around the Fermi level, as it was the case for the non-magnetic semiconductors in Ref. 20. The use of GW provides a direct band gap close to the K point which is slightly larger than the PBE calculated band gap, 0.427 eV with respect to 0.383 eV. Hence, V<sub>2</sub>TiSi can be classified as a narrow-band antiferromagnetic semiconductor. Although the energy gap is very small, the transition energies presented in Table II are very large, and away from the point in k-space, where the direct gap exists, large photon energies are needed to excite electrons, since the latter in the elastic regime conserve their **k**-value. The GW transition energies are smaller than the PBE ones contrary to the usual effect of quasiparticles on the band structure of semiconducting materials. This is also observed in other semiconductors like some non-magnetic semiconducting Heusler compounds.<sup>20</sup>

 $V_2$ ScP, contrary to  $V_2$ TiSi, exhibits a very narrow direct gap of 0.034 eV at the  $\Gamma$  point, while the transition energy at the X point is quite large (about 2 eV). The indirect  $\Gamma \to X$  and  $X \to \Gamma$  gaps are two thirds and one third of the  $X \to X$  transition energy, respectively. Therefore,  $V_2$ ScP can be classified as an almost-gapless semiconductor possessing a direct gap exactly at the  $\Gamma$  point.  $V_3$ Al within GW is found to be an almost-gapless semiconductor in agreement with previous calculations. Although its total DOS (not shown here) resembles that of  $V_2$ ScP, its band structure actually resembles that of  $V_2$ TiSi with a small direct gap between the K and  $\Gamma$  points. The width of the gap is 0.081 eV within PBE and slightly smaller (0.065 eV) within the GW. Transition energies for  $V_3$ Al are significantly larger than the band gap as was the case for  $V_2$ TiSi.

 $Cr_2ScAl$  and  $Co_2TiZn$  also show a semiconducting behavior. Their band structure resembles that of  $V_2TiSi$  in Fig. 3, but with a much flatter valence band near the  $\Gamma$  point.

For both compounds, we have an indirect gap with the minimum of the conduction band being located between the K and  $\Gamma$  points. The maximum of the valence band is exactly at the  $\Gamma$  point for  $Cr_2ScAl$  and between  $\Gamma$  and X for  $Cr_2TiZn$ . The band gap for both compounds is  $0.8-0.9\,eV$ . Thus, they should be classified as antiferromagnetic narrowband semiconductors. The GW self-energy correction gives larger band gaps and transition energies than PBE, contrary to what we have found for the V compounds, while being in accordance with the usual self-energy effect on the band structure of semiconductors.

The two Mn compounds show a different behavior. As obvious from Fig. 2, they are semimetals with a region of low DOS around the Fermi level. The Fermi level crosses both the conduction and valence bands creating electron and hole pockets. The bottom of the conduction band is 0.143 and 0.127 eV below the Fermi level for Mn<sub>2</sub>NaAl and Mn<sub>2</sub>MgZn, respectively (the PBE values are 0.174 eV and 0.106 eV). The transition energy at the  $\Gamma$  point is 0.628 eV and 0.548 eV for the two compounds, respectively (0.594 eV and 0.548 eV using PBE).

Finally, we have also calculated the Cr<sub>2</sub>ScAl and Cr<sub>2</sub>TiZn compounds assuming the so-called inverse (or XA or *Xa*) lattice structure where the sequence of the atoms changes with respect to the usual  $L2_1$  lattice structure; the sequence along the diagonal of the cube in Fig. 1 is now Cr-Cr-Sc(Ti)-Al(Zn). The inverse structure occurs usually when the valence of the Y atom in the X<sub>2</sub>YZ compound is larger than the valence of the X atoms. We found that the inverse structure is higher in energy with respect to the  $L2_1$  by  $0.1-0.2\,\mathrm{eV}$ , and thus the  $L2_1$  is energetically favorable. The Cr atoms, which are now nearest neighbors, possess large antiparallel spin magnetic moments slightly smaller than in the  $L2_1$  case, but now also the Sc(Ti) atoms possess considerable spin magnetic moments, which are parallel to the spin moments of the Cr atoms at the B sites and antiparallel to the spin moments of the Cr atoms at the A sites, similar to the situation occurring in other full-Heusler crystallizing in the inverse structure like Mn<sub>2</sub>CoAl.<sup>23</sup> The total spin magnetic moment slightly deviates from the zero value, and the compound is now a usual almost fully compensated ferrimagnetic half-metal with a low DOS in the spin-up band structure and a gap in the spin-down band structures instead of an antiferromagnetic semiconductor as in the  $L2_1$  structure.

#### IV. SUMMARY AND CONCLUSIONS

In conclusion, we have studied the quasi-particle band structure of several full-Heusler compounds with 18 (or 28 if Zn is present) valence electrons susceptible of being antiferromagnetic semiconductors. In all cases, the favorable magnetic configuration is the G-type antiferromagnetic one with large spin magnetic moments at the transition metal sites. Our results suggest that the V-based compounds (V<sub>3</sub>Al, V<sub>2</sub>ScP, and V<sub>2</sub>TiSi) and the Cr-based ones (Cr<sub>2</sub>ScAl and Cr<sub>2</sub>TiZn) are actually almost-gapless or narrow-gap semiconductors, while the Mn-based compounds (Mn<sub>2</sub>NaAl and Mn<sub>2</sub>MgZn) are semimetals. The *GW* approximation leads to band gaps and transition energies that do not deviate much

from the PBE ones. Thus, the standard DFT based first-principles calculations are reliable for describing the electronic and magnetic properties of these materials. We expect our results to further intensify the interest in antiferromagnetic spintronics and the use of Heusler compounds in this new research field.

# **ACKNOWLEDGMENTS**

The authors wish to thank Ş. Tırpancı for fruitful discussions.

- <sup>1</sup>E. V. Gomonay and V. M. Loktev, "Spintronics of antiferromagnetic systems," Low. Temp. Phys. **40**, 17 (2014).
- <sup>2</sup>T. Jungwirth, X. Marti, P. Wadley, and J. Wunderlich, "Antiferromagnetic spintronics," Nat. Nanotechnol. 11, 231 (2016).
- <sup>3</sup>Q. L. He *et al.*, "Tailoring exchange couplings in magnetic topological-insulator/antiferromagnet heterostructures," Nat. Mater. **16**, 94–100 (2016).
- <sup>4</sup>A. Hirohata and K. Takanashi, "Future perspectives for spintronic devices," J. Phys. D: Appl. Phys. 47, 193001 (2014).
- <sup>5</sup>Heusler Alloys. Properties, Growth, Applications, Springer Series in Materials Science Vol. 222, edited by C. Felser and A. Hirohata (Springer International Publishing, 2016).
- <sup>6</sup>I. Galanakis, P. H. Dederichs, and N. Papanikolaou, "Origin and properties of the gap in the half-ferromagnetic heusler alloys," Phys. Rev. B **66**, 134428 (2002).
- <sup>7</sup>I. Galanakis, P. H. Dederichs, and N. Papanikolaou, "Slater-Pauling behavior and origin of the half-metallicity of the full-Heusler alloys," Phys. Rev. B **66**, 174429 (2002).
- <sup>8</sup>S. Skaftouros, K. Özdoğan, E. Şaşıoğlu, and I. Galanakis, "Generalized Slater-Pauling rule for the inverse Heusler compounds," Phys. Rev. B 87, 024420 (2013).
- <sup>9</sup>K. Özdoğan, E. Şaşıoğlu, and I. Galanakis, "Slater-Pauling behavior in LiMgPdSn-type multifunctional quaternary Heusler materials: Halfmetallicity, spin-gapless and magnetic semiconductors," J. Appl. Phys. 113, 193903 (2013).
- <sup>10</sup>T. Graf, C. Felser, and S. S. P. Parkin, "Simple rules for the understanding of Heusler compounds," Prog. Solid State Chem. 39, 1 (2011).
- <sup>11</sup>C. Felser, G. H. Fecher, and B. Balke, "Spintronics: A challenge for materials science and solid-state chemistry," Angew. Chem., Int. Ed. 46, 668 (2007).
- <sup>12</sup>S. Wurmehl, H. C. Kandpal, G. H. Fecher, and C. Felser, "Valence electron rules for prediction of half-metallic compensated-ferrimagnetic behaviour of Heusler compounds with complete spin polarization," J. Phys.: Condens. Matter 18, 6171 (2006).
- <sup>13</sup>Ş. Tırpancı, E. Şaşıoğlu, and I. Galanakis, "Design of half-metallic Heusler-based superlattices with vanishing net magnetization," J. Appl. Phys. 113, 043912 (2013).

- <sup>14</sup>T. Graf, F. Casper, J. Winterlik, B. Balke, G. H. Fecher, and C. Felser, "Crystal structure of new Heusler compounds," Z. Anorg. Allg. Chem. 635, 976 (2009).
- <sup>15</sup>M. E. Jamer, G. E. Sterbinsky, G. M. Stephen, M. C. DeCapua, G. Player, and D. Heiman, "Magnetic properties of low-moment ferrimagnetic Heusler Cr<sub>2</sub>CoGa thin films grown by molecular beam epitaxy," Appl. Phys. Lett. 109, 182402 (2016).
- <sup>16</sup>I. Galanakis, Ş. Tırpancı, K. Özdoğan, and E. Şaşıoğlu, "Itinerant G-type antiferromagnetism in D0<sub>3</sub>-type V<sub>3</sub>Z (Z = Al, Ga, In) compounds: A first-principles study," Phys. Rev. B **94**, 064401 (2016).
- <sup>17</sup>See www.flapw.de for the description of the FLEUR code.
- <sup>18</sup>J. P. Perdew, K. Burke, and M. Ernzerhof, "Generalized gradient approximation made simple," Phys. Rev. Lett. 77, 3865 (1996).
- <sup>19</sup>C. Friedrich, S. Blügel, and A. Schindlmayr, "Efficient implementation of the *GW* approximation within the all-electron FLAPW method," Phys. Rev. B 81, 125102 (2010).
- <sup>20</sup>M. Tas, E. Şaşıoğlu, I. Galanakis, C. Friedrich, and S. Blügel, "Quasiparticle band structure of the almost-gapless transition metal based Heusler semiconductors," Phys. Rev. B 93, 195155 (2016).
- <sup>21</sup>S. Khmelevskyi, "First-principles modeling of longitudinal spin fluctuations in itinerant electron antiferromagnets: High Néel temperature in the V<sub>3</sub>Al alloy," Phys. Rev. B **94**, 024420 (2016).
- <sup>22</sup>M. E. Jamer, B. A. Assaf, G. E. Sterbinsky, D. Arena, L. H. Lewis, A. A. Saúl, G. Radtke, and D. Heiman, "Antiferromagnetic phase of the gapless semiconductor V<sub>3</sub>Al," Phys. Rev. B **91**, 094409 (2015).
- <sup>23</sup>S. Skaftouros, K. Özdoğan, E. Şaşıoğlu, and I. Galanakis, "Search for spin gapless semiconductors: The case of inverse Heusler compounds," Appl. Phys. Lett. **102**, 022402 (2013).
- <sup>24</sup>S. Ohshima, H. Ishida, T. Wakiyama, and K. Okuyama, "Self-epitaxial growth of metastable A15 V<sub>3</sub>Al on Au-coated sapphire substrates," Jpn. J. Appl. Phys., Part 1 28, 1362 (1989).
- <sup>25</sup>See http://www.oqmd.org for the Open Quantum Materials Database.
- <sup>26</sup>S. Kirklin, J. E. Saal, B. Meredig, A. Thompson, J. W. Doak, M. Aykol, S. Rühl, and C. Wolverton, "The Open Quantum Materials Database (OQMD): assessing the accuracy of DFT formation energies," npj Comput. Mater. 1, 15010 (2015).
- <sup>27</sup>I. Galanakis, K. Özdoğan, and E. Şaşıoğlu, "High- $T_{\rm C}$  fully-compensated ferrimagnetic semiconductors as spin-filter materials: The case of CrVXAl (X = Ti, Zr, Hf) Heusler compounds," J. Phys.: Condens. Matter **26**, 086003 (2014); Corrigendum: **26**, 379501 (2014).
- <sup>28</sup>G. M. Stephen, I. McDonald, B. Lejeune, L. H. Lewis, and D. Heiman, "Synthesis of low-moment CrVTiAl: A potential room temperature spin filter," Appl. Phys. Lett. **109**, 242401 (2016).
- <sup>29</sup>R. Skomski, Simple Models of Magnetism (Oxford University Press, 2008).
- <sup>30</sup>D. Jiles, Introduction to Magnetism and Magnetic Materials (Chapman & Hall, London, 1998).
- <sup>31</sup>J. Kübler, A. R. Williams, and C. B. Sommers, "Formation and coupling of magnetic moments in Heusler alloys," Phys. Rev. B 28, 1745 (1983).

